

Stable Levitation Control of Magnetically Suspended Vehicles with Structural Flexibility

Thomas E. Alberts, Grzegorz Oleszczuk, and Aravind M. Hanasoge

Abstract—This paper presents a simple analysis evaluating the stability threshold for magnetically levitated flexible structures using dissipative collocated controllers. It is shown that with such a control structure, the controller that stabilizes a rigid levitated mass can also stabilize a flexible structure with the same overall mass and electrodynamics. This principle has been experimentally demonstrated on flexible single and multi-magnet levitation systems.

I. INTRODUCTION

In the years 2001 to 2002, an experimental Maglev transportation system was installed on the Old Dominion University (ODU) campus by American Maglev Technologies (AMT). This system, which was intended to become a permanent student transportation system after one year of demonstration, never achieved fully operational status. The system was constructed on an aggressive schedule, and AMT reported encouraging results based on early testing in Florida. However, late in 2002 after installation of the system at ODU and some initial on-campus testing, the project came to a halt due technical difficulties in achieving stable levitation, and eventually budget overruns. Currently, the ODU Maglev system is used as a research vehicle by several of the University's engineering faculty.



Figure 1 ODU Maglev Vehicle on Guideway

Manuscript received September 14, 2007.

T. E. Alberts is a Professor of Aerospace Engineering at Old Dominion University, Norfolk VA 23529 USA. (757-683-3736; e-mail: talberts@odu.edu).

G. Oleszczuk, was with Old Dominion University, Norfolk VA 23529 USA. He is now with Honeywell Process Solutions, Warsaw POLAND, 39B02-672. (e-mail: grzegorz.oleszczuk@honeywell.com).

A.M. Hanasoge is with Old Dominion University, Norfolk VA 23529 USA. (e-mail: ahanasog@odu.edu).

The initial tests of the vehicle were conducted in Florida on a guideway mounted to the earth on a concrete foundation. In contrast, the ODU installation employed an elevated guideway using 90 foot long, essentially simply supported, girders of prestressed concrete construction. The inability to achieve stable levitation was attributed to flexibility of the guideway girders, and the widely accepted conclusion was that the guideway was simply too flexible to permit stable levitation. This paper sets out to dispel that notion using Routh stability analysis of a simplified magnetically levitated flexible structure.

II. STABILIZING SIMPLE RIGID MAGLEV SYSTEMS

A. Rigid Mass System

In its most fundamental form, attractive mode or EMS (Electro-Magnetic System) magnetic levitation can be simplified to a single magnet levitating a rigid mass as illustrated in Figure 2.

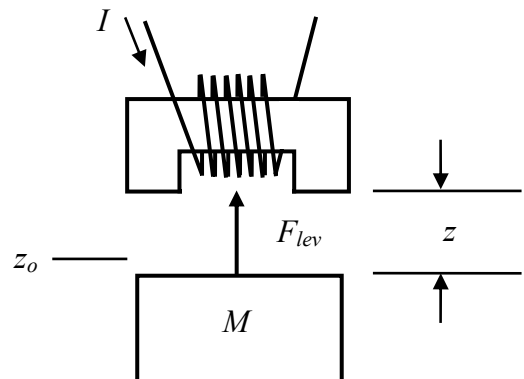


Figure 2 Levitation of a Simple Rigid Mass

In this figure, z represents the air gap between the mass and the magnet, and z_0 is a reference operating point for linearization. Current I is applied to the coils producing levitation force F_{lev} .

B. Fundamental modeling

The electromagnetic model employed in the following analysis corresponds to a U-shaped magnet interacting with a U-shaped rail as illustrated in Figure 3.

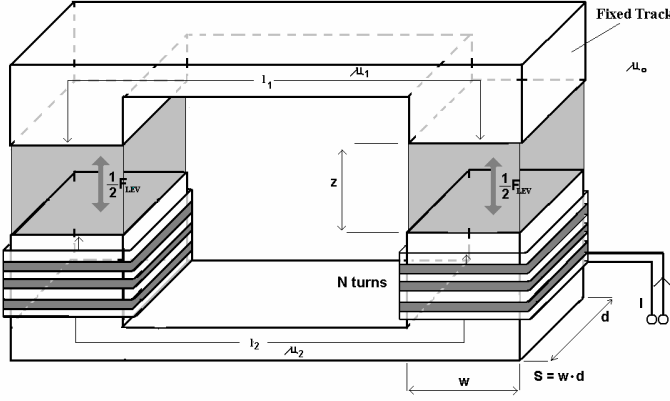


Figure 3 U-Shaped Magnet and Rail

For such a configuration, the electromagnetic force of attraction can be expressed as [1]:

$$F = \frac{1}{4} \frac{\mu_0 N^2 I^2 w d}{z^2} \left\{ 1 + \frac{2z}{\pi \cdot w} \right\} \quad (1)$$

In this expression, which was simplified due to assuming zero lateral offset, the symbols μ_0, d, N, w represent respectively permeability, coil length, number of turns, and width of the coil and variables z , and I represent air gap and current. The inductance of the magnet is expressed as:

$$L(z) = \mu_0 N^2 d \left[-\frac{w}{2z} - \frac{1}{\pi} \ln\left(\frac{1}{z}\right) \right] \quad (2)$$

C. Linearization

For further analysis, the force expression can be linearized [2] with respect to reference values for gap z_0 and current I_0 , using the first derivative components from the Taylor series expansion:

$$F \cong F|_{z_0} + \frac{\partial F_{LEV}}{\partial z} \Big|_{z_0} (z - z_0) + \frac{\partial F_{LEV}}{\partial I} \Big|_{I_0} (I - I_0) \quad (3)$$

Thus a linear expression for the electromagnetic force is as follows:

$$F \cong -k_z z + k_i I \quad (4)$$

where:

$$k_i = \frac{1}{2} \frac{\mu_0 N^2 I_0 w d}{z_0^2} \left(1 + 2 \frac{z_0}{\pi \cdot w} \right) \quad (5)$$

$$k_z = \frac{1}{2} \frac{\mu_0 N^2 I_0^2 w d}{z_0^3} \left(1 + 2 \frac{z_0}{\pi \cdot w} \right) - \frac{\mu_0 N^2 d I_0^2}{2\pi \cdot z_0^2} \quad (6)$$

Electromagnets are typically driven by current amplifiers intended to follow a current command I^{Cmd} , with is a current feedback gain K_a . Based on this model, the governing equation of the electromagnetic circuit is expressed as:

$$\frac{dI}{dt} = \frac{I^{Cmd} K_a - I(K_a + R)}{L(z)} + \frac{k_z}{k_i} \dot{z} \quad (7)$$

In (7), R is the resistance of the magnet coils, and $L(z)$ is the coil inductance defined previously. Note the presence of a back EMF term with gain k_z/k_i . For simplicity we assume

that $L(z) = L = \text{Constant}$ near the nominal operating point of $z = z_0$.

D. Model of a Simple Levitated Rigid Mass

Consider a simple one-degree-of-freedom rigid model of the maglev system as shown in Figure 2. Equations of motion for the system can be expressed as:

$$\frac{d^2 z}{dt^2} = \frac{k_z}{M} z - \frac{k_i}{M} I \quad (8)$$

Using the standard state-space [3] form (9), the equations of motion for the rigid system are expressed as shown in Equations (10) and (11).

$$\begin{aligned} \dot{\vec{x}} &= A \cdot \vec{x} + B \cdot \vec{u} \\ \vec{y} &= C \cdot \vec{x} + D \cdot \vec{u} \end{aligned} \quad (9)$$

$$\begin{bmatrix} \dot{z} \\ \ddot{z} \\ \dot{I} \end{bmatrix} = \begin{bmatrix} 0 & 1 & 0 \\ \frac{k_z}{M} & 0 & -\frac{k_i}{M} \\ 0 & \frac{k_z}{k_i} & -\frac{(K_a + R)}{L} \end{bmatrix} \begin{bmatrix} z \\ \dot{z} \\ I \end{bmatrix} + \begin{bmatrix} 0 \\ 0 \\ \frac{K_a}{L} \end{bmatrix} I^{Cmd} \quad (10)$$

$$\begin{bmatrix} z \\ \dot{z} \\ I \end{bmatrix} = \begin{bmatrix} 1 & 0 & 0 \\ 0 & 1 & 0 \\ 0 & 0 & 1 \end{bmatrix} \begin{bmatrix} z \\ \dot{z} \\ I \end{bmatrix} \quad (11)$$

Note that the characteristic polynomial of A (10) is as follows:

$$|sI - A| = s^3 + \alpha s^2 - \frac{k_z}{M} \alpha \quad (12)$$

Based on (10) and (11) the transfer function can be calculated:

$$G_R(s) = \frac{-K_x}{s^3 + \alpha s^2 - \frac{k_z}{M} \alpha} \cong \frac{-K_x}{(s-p)(s+p)(s+\alpha)} \quad (13)$$

where:

$$p = \sqrt{\frac{k_z}{M}}, \quad \alpha = \frac{K_a + R}{L}, \quad K_x = \frac{K_a k_i}{M L} \quad (14)$$

When $\alpha \gg \sqrt{\frac{k_z}{M}}$, which is generally the case, then the approximation of (13) is quite accurate.

The system has three real poles. One is positive, which is indicative of the inherent instability of EMS maglev systems. The pole α is associated with the electrical characteristics of the magnet and current feedback. The real pair $\pm p$ replaces the rigid body poles of the purely structural model. The value of p can vary significantly with gap and current.

III. STABILIZING SIMPLE MAGLEV SYSTEMS

It is a simple matter to show that the stabilization of the single rigid mass structure can be accomplished using a PD

compensator with positive gap feedback. Let the compensator have the form:

$$C_o(s) = K_p + K_D s \quad (15)$$

The feedback structure considered is as shown in Figure 4, where negative feedback is initially assumed.

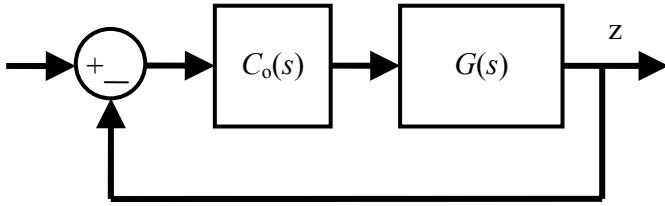


Figure 4 Basic Feedback Structure

The PD compensator is an example of a dissipative controller [4]. When used in a simple feedback loop for a single magnet to control the variation of its own air gap, then it is called decentralized [5].

Based on the considerations above, the closed-loop transfer function for the rigid single mass system under PD control is:

$$G_R^{CL}(s) = \frac{-K_x(K_p + K_D s)}{s^3 + s^2 \alpha - s K_x K_D - (p^2 \alpha + K_x K_p)} \quad (16)$$

The CL superscript designates closed-loop. The sufficient conditions for the stability of this system are determined using the Routh criterion [3], which produces the following conditions:

$$K_p < \frac{-p^2 \alpha}{K_x}, \quad K_D < \frac{K_p}{\alpha} + \frac{p^2}{K_x} \quad (17)$$

These conditions indicate the necessity for strictly negative gains K_p and K_D , in other words positive feedback, and moreover, that the gains have a minimum threshold magnitude for stability. Further, the satisfaction the first part of (17), the condition on K_p , leads to $K_D < 0$.

A. Maglev as a simple flexible system

As a first step toward evaluation of the impact of structural flexibility on control of a maglev system, a single flexible mode is introduced. Note that from a dynamics perspective, this mode could equivalently represent either guideway or vehicle flexibility. The new structural model is shown schematically in Figure 5.

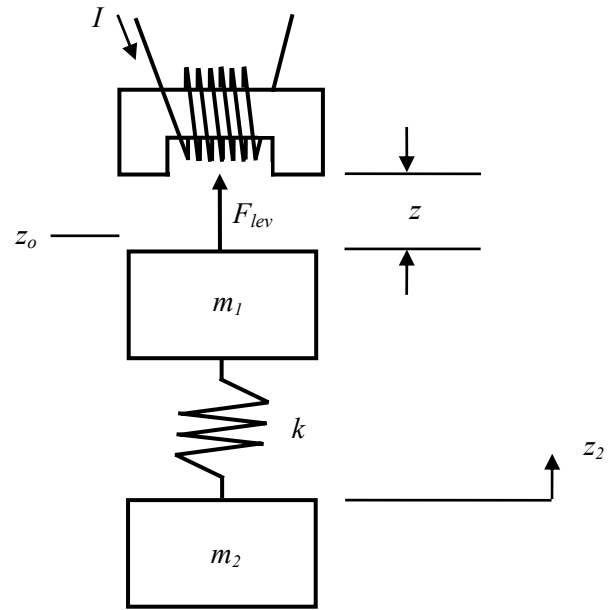


Figure 5 Simple Flexible Structure Maglev System

In this system $m_1 + m_2 = M$ still represents the overall weight of the initial system. The actuator model equation (7) remains the same. The spring constant k represents structural flexibility. The displacement resulting from structural flexibility is denoted by z_2 , while the electromagnetic air gap is denoted by z . The new equations of motion become:

$$\frac{d^2 z}{dt^2} = \frac{k_z - k}{m_1} z + \frac{k}{m_1} z_2 - \frac{k_i}{m_1} I \quad (18)$$

$$\frac{d^2 z_2}{dt^2} = \frac{k}{m_2} z - \frac{k}{m_2} z_2 \quad (19)$$

$$\frac{dI}{dt} = \frac{I^{Cmd} K_a - I(K_a + R)}{L} + \frac{k_z}{k_i} \dot{z} \quad (20)$$

Similar to the notation of the rigid case, the following notation is introduced:

$$\omega_1^2 = \frac{k}{m_1}, \quad \omega_2^2 = \frac{k}{m_2}, \quad \tilde{p}^2 = \frac{k_z}{m_1} \quad (21)$$

In state equation associated with these equations can be expressed as:

$$\begin{bmatrix} \dot{z} \\ \dot{z}_2 \\ \ddot{z} \\ \ddot{z}_2 \\ \dot{I} \end{bmatrix} = \begin{bmatrix} 0 & 0 & 1 & 0 & 0 \\ 0 & 0 & 0 & 1 & 0 \\ \tilde{p}^2 - \omega_1^2 & \omega_1^2 & 0 & 0 & -\frac{k_i}{m_1} \\ \omega_2^2 & -\omega_2^2 & 0 & 0 & 0 \\ 0 & 0 & \frac{k_z}{k_i} & 0 & -\alpha \end{bmatrix} \begin{bmatrix} z \\ z_2 \\ \dot{z} \\ \dot{z}_2 \\ I \end{bmatrix} + \begin{bmatrix} 0 \\ 0 \\ 0 \\ 0 \\ \frac{K_a}{L} \end{bmatrix} I^{Cmd} \quad (22)$$

The C matrix of the state-space representation (9) depends upon the sensor locations. When the actuator and sensor pairs are located together, the pair is said to be collocated [4]. With regard to the present system, the collocated case has C matrix:

$$C_c = [1 \ 0 \ 0 \ 0 \ 0] \quad (23)$$

The so-called non-collocated¹ case, in which the input is applied to mass m_1 and the output is measured from mass m_2 has:

$$C_n = [0 \ 1 \ 0 \ 0 \ 0] \quad (24)$$

The D matrix is zero for either case. Applying the standard transformation from state-space to transfer function form, the open-loop transfer function for collocated plant is:

$$G_c(s) = \frac{-\tilde{K}_x(s^2 + \omega_2^2)}{\Delta(s)} \quad (25)$$

where:

$$\Delta(s) = s^5 + s^4\alpha + s^3(\omega_1^2 + \omega_2^2) \dots + s^2\alpha(\omega_1^2 + \omega_2^2 - \tilde{p}^2) - \tilde{p}^2\omega_2^2 \quad (26)$$

and:

$$\tilde{K}_x = \frac{K_a k_i}{m_1 L} \quad (27)$$

The open-loop transfer function for non-collocated plant is:

$$G_n(s) = \frac{-\tilde{K}_x\omega_2^2}{\Delta(s)} \quad (28)$$

As in the rigid case, it is observed that these transfer functions are unstable and non-minimum phase. For the non-collocated case there are no zeros, a condition that makes the system more difficult to stabilize because it has lower relative degree.

Considering each of these systems in a feedback loop such as Figure 2, and performing a similar Routh analysis, one can evaluate and compare the stability conditions.

B. PD Control of the Collocated Flexible System

Under PD control, the closed-loop characteristic polynomial for the collocated flexible system (25) is as follows:

$$\Delta^{cl}(s) = s^5 + \alpha s^4 + (\omega_1^2 + \omega_2^2 - K_D \tilde{K}_x) s^3 \dots + (\alpha(\omega_1^2 + \omega_2^2 - \tilde{p}^2) - K_p \tilde{K}_x) s^2 \dots - K_D \tilde{K}_x \omega_2^2 s - \tilde{p}^2 \omega_2^2 \alpha - K_p \tilde{K}_x \omega_2^2 \quad (29)$$

Here the CL superscript designates closed-loop, and the subscript designates collocated. Upon inspection, it is immediately clear that the feedback gains must be negative for stability. Routh array analysis of the closed-loop collocated system yields the following sufficient conditions for stability:

$$K_p < \frac{-\tilde{p}^2 \alpha}{\tilde{K}_x} \equiv \frac{-p^2 \alpha}{K_x}, \quad K_D < \frac{K_p}{\alpha} + \frac{\tilde{p}^2}{\tilde{K}_x} \equiv \frac{K_p}{\alpha} + \frac{p^2}{K_x} \quad (30)$$

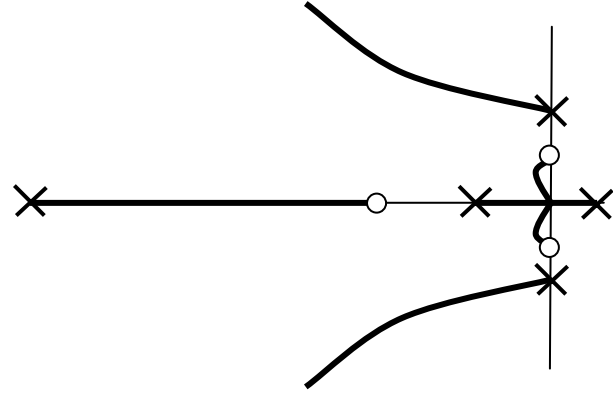
Thus it can be concluded that the exact same compensation that stabilizes the rigid system, will also stabilize the flexible

¹ Since the system considered has only 2 masses, this is an extreme example of non-collocation. Actual system with approximate collocation may be more forgiving

system. As in the rigid body case, the satisfaction the first part of (30) leads to $K_D < 0$.

The root locus diagram of Figure 6 illustrates typical stabilization of the collocated system using PD control. Note that, for a fixed compensator zero location (fixed K_D), the system is stable for all values of K_p less than the critical value identified in (30).

Figure 6 Root Locus of the PD Controlled Collocated System



C. PD Control of the Non-Collocated System

If one evaluates the denominator of the non-collocated system's closed-loop transfer function, it is found that in contrast to the collocated case, only the zero degree and first degree terms are influenced by the controller.

$$\Delta_n^{cl}(s) = s^5 + \alpha s^4 + (\omega_1^2 + \omega_2^2 - \tilde{p}^2) s^3 \dots + \alpha(\omega_1^2 + \omega_2^2 - \tilde{p}^2) s^2 - K_D \tilde{K}_x \omega_2^2 s \dots - \tilde{p}^2 \omega_2^2 \alpha - K_p \tilde{K}_x \omega_2^2 \quad (31)$$

Moreover, unlike in to the collocated case, a necessary condition for stability is that:

$$\omega_1^2 + \omega_2^2 > \tilde{p}^2 \Rightarrow k \left(1 + \frac{m_1}{m_2} \right) > k_z \quad (32)$$

which is usually satisfied in practice. More critically, the s^3 term in the first column of the Routh table is zero, indicating that the system can be marginally stable at best under PD control², thus a PD compensator is unable to stabilize the system. Interestingly, the remaining terms indicate that the requirements for marginal stability are the same as the stability requirements (17) for the collocated case.

IV. EXPERIMENTS

A. Single DOF Test Rig

A single degree of freedom test rig was constructed using

² Not necessarily the case in actual system with non-zero damping and with approximate collocation

one magnet and a short section of rail from the Old Dominion University Maglev system [6]. The magnet is capable of producing about 6000 lbs of lift force. The magnet is fixed in place and a section of track is suspended overhead from a lever arm, via a 4-bar linkage that allows vertical movement of the track, but keeps it aligned with the magnet. Weights are hung from the far end of the lever arm with a 4 to 1 mechanical “disadvantage,” such that the magnet(s) have to produce 4,000 pounds of attractive force to lift 1,000 pounds for example. The rig is fitted with load cells to measure vertical and lateral load. The lever arm can be locked in place using screw jacks to permit static testing of the magnets, for example to verify magnet force plots. An eddy current based sensor is used for gap measurement.

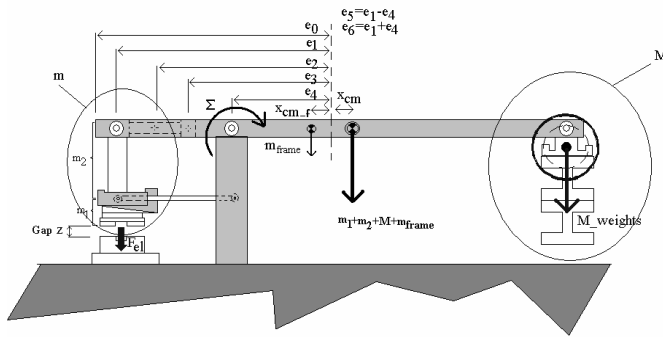


Figure 7. Simple Schematic of the Maglev Test Rig

The test rig was designed to exhibit structural flexibility representative of a full scale system. For lumped parameter analysis, a simplified representation of the system’s flexibility was considered. In effect, this model simplifies the structure to three point masses connected by two discrete springs as illustrated in Figure 8.

Bode plots for a collocated (based on mass 1) and non-collocated (output at mass 2) model of the system are given in Figure 9. It can be seen that the non-collocated case is similar to collocated, with the exception that the pair of zeros at 80Hz is not present in the non-collocated case. This is similar to the simple two mass example presented earlier. Note that this plot represents the “levitated” case, that is, when the entire system is floating in space.

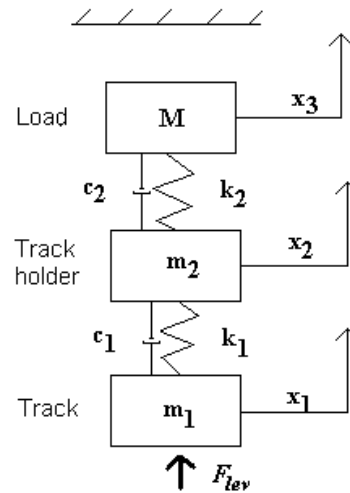


Figure 8. Three Mass Model of the Test Rig

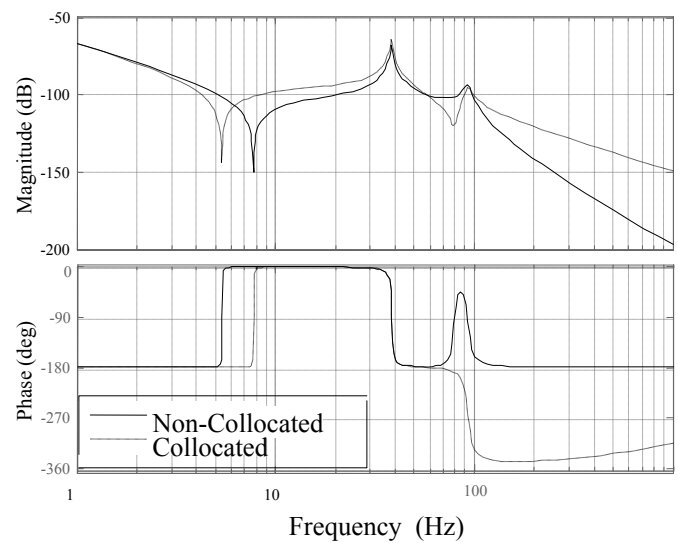


Figure 9. Analytical Bode Plots for the Levitated Test Rig

In practice, it was not practical to experimentally validate the model represented in Figure 9. Instead, the open-loop model of the non-levitated case was verified. This corresponds to the load M resting on the ground, in effect locking it in place which would be equivalent to setting x_3 to zero.

A Hewlett Packard dynamic signal analyzer was used to verify this case using 3 different air gap settings. The test was performed by driving the magnet current with a sine sweep input while monitoring the air gap reading. The analytical and experimental results were found to be in close agreement as shown in Figure 10.

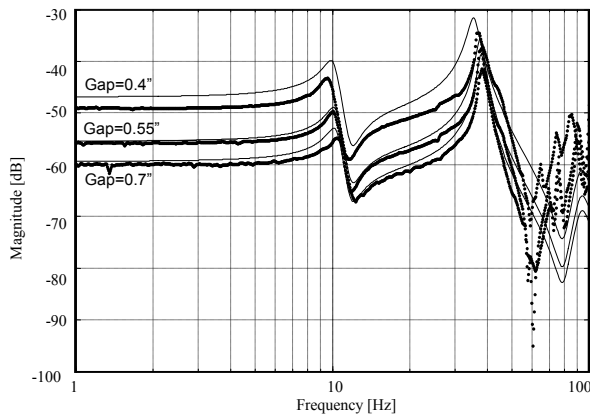


Figure 10 Experimental and analytical data for three different cases gap $z = 0.4$, $z = 0.55$, and $z = 0.7$ [in] (Thin solid lines are analytical)

B. Levitation Control of the Test Rig

Numerous successful levitation experiments have been conducted using the ODU single degree of freedom test rig. Controllers are implemented using a Matlab[®] application known as xPC Target[®]. With this application, a compensator constructed graphically using Matlab's Simulink[®] environment on a host computer, can be converted to C-code and compiled, then uploaded to the target machine. In this particular test configuration a desktop PC computer was used as a host. A PC104 single based computer with Intel 468 series processor was used as a target. Communication between these two devices was established via Ethernet. The PC104 computer was equipped with a PCI based National Instruments data acquisition card. The sample rate for was set to 20 kHz. The high sample rate was used to allow over-sampling of the measurements so that digital filters could be used to help reduce signal noise.

Typically, to obtain acceptably stable results, controller designs had to be slightly more conservative in terms of gain and phase margin than analysis suggested. It is believed that this was primarily due to discrete time implementation, the presence of anti-aliasing filters, and electromagnetic non-linearities.

In the interest of brevity, the experimental implementation is not exhaustively covered here; however a typical result is presented in Figure 11. The controller was designed as a PD controller, based on the principles described in this paper. After suitable performance was achieved, a low gain error integrator term was added to reduce steady state error. The commanded gap value was 0.4\".

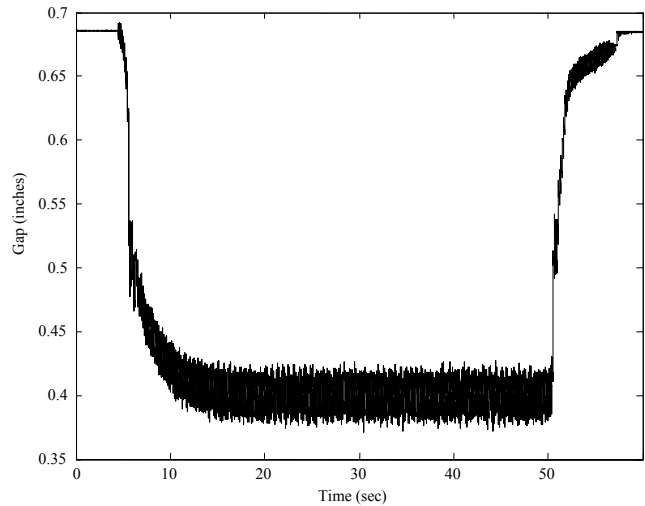


Figure 11. Typical Test Rig Levitation Using PID Control

V. CONCLUSIONS

This paper has presented simple analysis to explore the stability of maglev systems with structural flexibility. Although not discussed exhaustively in this paper, the results can be extended to more complex flexible systems. Initial results with a single degree of freedom test rig corroborate the analytical results. The main conclusion is that PD control can always stabilize a flexible maglev system providing that actuators and sensors are collocated, and subject to these restrictions and providing that the mass and electrodynamic are the same the exact same compensator that stabilizes a rigid maglev structure will also stabilize the corresponding flexible structure. These principles have been successfully demonstrated on a single magnet laboratory test rig, a 5000 pound 6 magnet laboratory test bogie, and finally on the full scale 12 magnet ODU maglev on the elevated guideway.

REFERENCES

- [1] Limbert, A., Richardson, H.H. & Wormley, D.N. 1976. Controlled Dynamic Characteristics of Ferromagnetic Vehicle Suspension Providing Simultaneous Lift and Guidance. *Journal of Dynamics Systems, Measurement, and Control* 101: 217-222
- [2] Goodall, R.M. 1985. The theory of electromagnetic levitation. *Physics in Technology* 16(5): 207-21
- [3] Ogata, K. 1970. *Modern Control Engineering*. Prentice-Hall.
- [4] Joshi, S.M. 1989. *Control of Large Flexible Space Structures*, Springer Verlag.
- [5] West-Vukovich, G.S. & Davison, E.J. 1984. The Decentralized Control of Large Flexible Space Structures, *IEEE. Automatic Control*. 29(10): 866-879.
- [6] Davey, K., Morris, T., Britcher, C., Tola, R. & McCune, M. 2001. The Old Dominion University/American Maglev Demonstration System. *6th International Symposium on Magnetic Suspension Technology*, Turin, Italy.